COPING WITH WAKE VORTEX

Klaus-Uwe Hahn
Institute of Flight Research, German Aerospace Center (DLR)
Lilienthalplatz 7, 38108 Braunschweig, Germany

Keywords: *wake vortex, encounter, control, safety, separation distance*

Abstract

The well known phenomenon of wake vortices behind a lift producing wing can adversely affect flight safety if encountered by trailing aircraft. The strength of the vortices increases with the weight of the vortex generating aircraft. Therefore, weight dependent separation distances have been established for approach and landing to avoid dangerous wake vortex encounters. These proven separation distances have to be investigated carefully with the aim to discover possible margins to be used to solve the current and future capacity problems at airports. This demand forms the need for more flexible separation procedures taking into account the actual weather situation and the parameters of the individual aircraft pairing. Separation reductions can be achieved by wake vortex avoidance using prediction systems for the wake vortex development and movement. The hazardous areas around a wake vortex can be approximated by the simple geometry of a rectangle or an ellipse according to the aircraft pairing, the actual weather dependent decay and the available control power for vortex compensation. Using specific controllers vortices can be passed through even if the required control power temporarily exceeds the available capacity. Aircraft equipped with such a controller might follow another aircraft closer than authorized by the current separation distances.

List of Symbols and Abbreviations

AVOSS	Aircraft Wake VOrtex Spacing System
b	wing span
DoF	degrees of freedom
DLR	German Aerospace Center
G	aircraft weight
IMC	instrumental meteorological conditions
MTOW	maximum take-off weight
nm	nautical mile
P2P	probabilistic two phase model
r	radius / radial co-ordinate
ROT	runway occupation time
s	spanwise load factor
SD	separation distance
t	time co-ordinate
T	thrust, time constant
v	lateral velocity component
V	airspeed (no index), velocity
w	vertical velocity component
W	weight
α	angle of attack
β	angle of sideslip
χ	flight path azimuth
γ	flight path angle
η	elevator deflection
ν	effective viscosity
ρ	air density
ξ	aileron deflection
ζ	rudder deflection
Δ	difference
Φ	bank angle
Θ	pitch angle
ψ	azimuth
indices	
c	core
F	follower aircraft
FB	feedback
FF	feed-forward
g	geodetic
K	kinetic (refers to flight path)
L	leading/generator aircraft
req	required
sink	indicates downwards motion
t	tangential
W	wind
WV	wake vortex
WVL	wake vortex line
$\dot{}$	time derivative
'	characteristic time scale
*	denotes normalized parameters
0	initial value
1	diffusion phase
2	rapid decay phase

1 Introduction

As a reaction to the generation of lift, two counter rotating vortices arise at the wing tips of an aircraft. This phenomenon is well known as wake vortex and can adversely affect flight safety of trailing aircraft. This is particularly true if a light aircraft follows a heavy one since the strength of the generated vortices depend on the required lift correspondingly to the aircraft weight. To avoid dangerous vortex encounters the aircraft staggering for approach and landing is restricted. The allowed minimum separation is a limiting factor for airport capacities. The current and the expected capacity problems at airports with a high volume of traffic together with future large and very heavy aircraft form the need for a revision of the existing rigid separation concepts. This demand has led to a new interest and comprehensive investigations into the nature of the wake vortex phenomenon.

The following investigation and the presented simulation results will focus on the combination of a small aircraft following behind a large one. For this encounter situation real flight test data have been available for validation. The drawn conclusions are of general importance since the underlying physics are true for any aircraft combinations.

The effects of wake vortices on aircraft can be very different. Encounters perpendicular to the vortex axis will lead to substantial vertical load factor variations by inducing rapid and large angle of attack variations all over the wing [1] comparable to strong gusts. Another situation is present if the flight path of the encountering aircraft runs parallel to the vortex axis. Then the vortex flow will induce varying angles of attack along the wing producing strong rolling moments which can create significant roll rates resulting in large bank angles. Between these two cases a broad variety of encounter situations exists. In any case the wake vortex produces an adverse effect on aircraft motion which is the reason for the today's encounter avoidance policy. The pilots position concerning wake vortex is formulated by the statement that no aircraft should encounter a wake vortex by intention whatever its strength is.

Presuming approaches on a single runway where small encounter angles $\psi \approx \psi_L \approx \psi_{WVL}$ can be assumed, normally the situation of a parallel-like encounter will prevail. The investigated scenario is sketched in Fig.1.

2 Wake Vortex Spacing of Aircraft

2.1 Fixed Aircraft Separation Distances

To guarantee safe flight operation, currently fixed mass dependent separation distances have been established for aircraft lined up for approach and landing. Various matrices of minimum separation distances from different organizations are available. Tab.1 gives the mass classification of aircraft and in Tab.2 the corresponding IMC vortex separations after FAA are listed. Such fixed matrices can be easily applied to flight operation. But they suffer from the lack of flexibility to actual ambient weather situation.

2.2 Dynamic Aircraft Separation

To reduce the current rigid separations research activities [2, 3, 4] have been initiated for the development of concepts for dynamic wake vortex spacing systems. The most mature system is the AVOSS for which already performance validations are carried out [5]. All activities finally aim for the increase of the aircraft throughput to improve airport capacity. The principle of dynamic spacing is based on the consideration of all relevant influences:

- *weather forecast* improved and updated by
- *sensing the ambient weather* conditions used together with
- *data of aircraft pairing* to
- *predict the vortex behavior* to provide a
- *non-hazardous vortex or vortex free space*

along the approach path. To overcome the uncertainties in the predictions adequate margins have to be introduced. The required time to guarantee a safe approach for a following aircraft (due to vortex demise or vortex drifting away) defines the minimum separation distance. To minimize the required separation actions can be taken to push the distances to their (safe) limits:

- measures to reduce vortex strength
- passive or active devices to speed up the vortex decay
- more precise prediction of vortex behavior
- minimization of the non-hazardous vortex or vortex free space
- active aircraft encounter control

Contributions have to come from aerodynamics, fluid dynamics and meteorology aiming for low vortex design, accelerated decay, weather and vortex behavior prediction. Another potential is available coming from aircraft control.

The use of an autopilot will improve the accuracy of flight path tracking [6]. A precise flight path tracking of the vortex generating aircraft reduces the scatter in position deviations around the nominal approach path and thus reduces the extension of the space in which the generation of vortices have to be expected (→ reduced uncertainty of initial vortex position). A more precise flight path tracking of the following aircraft shrinks the extension of the space which will be probably penetrated due to excursions from nominal path (→ reduced space of interest of vortex contamination). Therefore, it can be stated that the application of automatic approach will help to minimize two sources of probabilistic uncertainties.

Automatic control can also improve the aircraft response to a wake vortex encounter which might happen unintended. Accepting that the hazard of a wake vortex penetration results from the very dynamic response of the aircraft then the situation can be treated like a flight in strong turbulence which can be improved by a gust load alleviation system [7, 8]. The use of a vortex controller (of course controlling the aircraft response and not the encountered vortex itself) will shift the limits for a non-hazardous vortex situation to a higher level of acceptable vortex strength. Consequently, regarding the aircraft actual pairing and the available control power provided by the penetrating aircraft the separation distance can be further reduced. In any case the wake vortex encounter has to be safe in terms of acceptable flight path excursions and flight state deviations. The investigations into controlled wake vortex encounters have been performed in the frame of DLR's "Wirbelschleppe" project [3] by means of a realistic and detailed simulation program.

3 Data Gathering from Flight Tests

For the validation of a reliable wake vortex encounter simulation real flight test data have been used. The respective flight tests have been performed in the frame of the European S-Wake project within flight experiments especially designed for wake vortex encounter analyses [9]. In the following a brief description of the tests for the data gathering will be given.

As a vortex generating aircraft DLR's twin engine jet VFW614 ATTAS (**A**dvanced **T**echnologies **T**esting **A**ircraft **S**ystem) was used (Fig. 2). Having a MTOW of about 20 tons this aircraft has to be classified as "LARGE" following the classification of Tab.1. The test aircraft was equipped with a smoke generator on its left wing (Fig.3) to mark the vortex at the tip. This made it easy for the follower aircraft to encounter the vortex by intention.

The encountering aircraft was the Do 128 test aircraft of the Technical University of Braunschweig powered by two turbo-prop engines (Fig.4). With a maximum MTOW of about 4.35 tons the aircraft has to be classified as "SMALL". This aircraft was ideally suited for the encounter trials providing very high accuracy air data probes at 4 different stations allowing multipoint scans when passing the wake vortex. Numerous scans of encounters have been performed at various distances (between about 0.5nm and 1.5nm) during flight test campaigns in late summer 2001 and in early 2002. The recorded data have been analyzed by means of a parameter identification method to validate the mathematical models representing the wake vortex flow field and the encounter behavior.

4 Modeling and Simulation

The simulation system used for the investigation consists of various sub-models. The available modules and the data flow are shown in Fig.5. In the following the used main modules will be roughly introduced. For the choice of models

the rule “as complex as necessary but as simple as possible” was applied.

4.1 Aircraft Modeling

4.1.1 Vortex Generating Aircraft

The vortex generating aircraft was simply modeled by the wake vortex produced by itself. The common approach for the calculation of the strength of a fully developed single vortex is

$$\Gamma_0 = \frac{W_L}{2 \cdot \rho \cdot V_L \cdot b_L \cdot s} \qquad (1)$$

The term

$$b_0 = b_L \cdot s \qquad (2)$$

is the distance between the two vortex lines since the position of the trailing vortices are not exactly located at the wing tips. It can be assumed that $s = \pi/4$ applies if no specific data are available. These relations are well accepted in the community of wake vortex research and have been confirmed by the flight test data.

4.1.2 Encountering Aircraft

The encountering aircraft was modeled being a rigid body with full 6 DoF. The rigid body aerodynamics and the engine model were provided by the Institute of Flight Guidance from the Tech. Univ. of Braunschweig [10, 11].

The effect of the wake vortex flow induced supplementary angle of attack was considered following the approach of the ONERA strip model [12]. This model calculates the forces and moments from the local angle of attack variations computed at different sections, so called strips along the wing and along the horizontal stabilizer.

The encounter model was validated by a parameter identification method applied to the flight test data [13]. The results show that the model can be regarded to be a good approach in terms of realistic encounter representation.

4.2 Wake Vortex Modeling

4.2.1 Vortex Decay and Movement

For the velocity field behind a vortex generating aircraft the strength of the circulation Γ_L as a function of the time co-ordinate is the most important factor. Manifold models for the mathematical description of the vortex decay are available [14, 15, 16, 17] showing considerable different results.

A new approach for the wake vortex decay is proposed by HOLZÄPFEL [18]. This model is ideally suited for the use in flight mechanics simulations. This P2P model is a probabilistic parametrical model considering two different phases of vortex decay (Fig.6). First the diffusion phase followed by the second phase showing a rapid decay. The P2P model considers the relevant aircraft and atmospheric data determining the wake vortex behavior. The model delivers the time dependent strength of the vortices and their positions. Accepting that it will not be possible to get exact results from any model the P2P model uses a probabilistic component which gives uncertainty bounds of the spatial and temporal variations covering the expected vortex behavior. The model is checked against real data sets, e.g. the Memphis data [19] showing good correspondence (see Fig.7). For more details about this model it is referred to [18].

4.2.2 Vortex Velocity Field

From the circulation of the vortex the corresponding velocity field can be calculated. Again there are numerous approaches [20-24] available transforming the circulation Γ_L of a completely developed vortex into a radial dependent velocity distribution. In [13] it is shown that the best fit of a continuous model compared with real flight test data is obtained by the approach of BURNHAM and HALLOCK [22]

$$V_t = \frac{\Gamma_L}{2 \cdot \pi \cdot b_L} \cdot \frac{r^2}{r_c^2 + r^2} \,. \qquad (3)$$

This approach is able to produce a good match of the overall radial velocity shape. Corresponding to the two phase vortex decay the growth of the core radius r_c expressed by the normalized core radius r_c^* with

$$r_c = r_c^* \cdot b_0 \qquad (4)$$

is considered to have also two phases [25]:

$$t^* \le T_2^* : \quad r_c^* = r_{c0}^* \qquad (5)$$
$$t^* > T_2^* : \quad r_c^* = r_{c0}^* + \sqrt{\nu_2^* \cdot \left(t^* + T_2^*\right)} - \sqrt{2 \cdot \nu_2^* \cdot T_2^*}$$

ν_2^* is the normalized effective viscosity and applicable for the rapid decay phase, T_2^* is the normalized time when this phase starts and t^* is the normalized time coordinate calculated by

$$t^* = t / t' \qquad (6)$$

based on the characteristic time scale

$$t' = \left(2 \cdot \pi \cdot b_0^2\right) / \Gamma_0$$

The initial core radius for the fully developed vortex is r_{c0}. Also from parameter identification it was found out [13] that the core radius r_{c0} needs to be chosen smaller than given by the common estimate $r_c \approx 0.05\ b_L$. As a good approach it can be assumed that

$$r_{c0} \approx 0.035 \cdot b_L \qquad (7)$$

applies. The maximum tangential velocity at the core radius was identified to match that one coming from the LAMB-OSEEN model in combination with $r_c \approx 0.05$. This outcome fits perfectly to the factor of 0.035 used in Eq.(7) affecting the radial distribution of the velocity field after Eq.(3) and thus the maximum velocity at core radius. The time dependent development of the core radius described by Eqs.(5) and (7) is shown in Fig.8.

4.2.2 Wake Vortex Flow

For the complete wake vortex flow behind the leading aircraft a pair of counter rotating vortices one for each wing tip are superimposed. The distance between the two vortex lines b_0 is defined by Eq.(2). Looking into the direction of flight the left wing vortex is clockwise rotating. Fig.9 illustrates the result of this wake vortex model compared with data from in-flight measurement.

4.3 Encounter Control

4.3.1 Autopilot

To keep the aircraft on the desired approach path it needs to be controlled. The used autopilot is based on a model following concept [26]. This provides that the aircraft follows a (smooth) predefined angular state command model representing a realistic aircraft behavior. The main control is performed by feed-forward based on an inverse aircraft model. Unmodeled real world effects in the applied inverse vehicle model cause model following errors that have to be compensated by feedback. The block diagram of the autopilot is shown in Fig.10. The autopilot was designed to have a good performance in strong turbulence and gusts.

4.3.2 Autothrottle

For the thrust control a simple autothrottle (Fig.10) is used based on the total energy management of the aircraft [27, 28]. The required energy state for the steady flight is described by the airspeed V and the flight path angle γ. Any deviations from this reference state formulate the required thrust variation to reestablish the nominal situation. It applies

$$\Delta T = -\left(\dot{V}/g + \Delta\gamma\right) \cdot W \qquad (8)$$

where W is the aircraft's weight. From the demand for thrust the throttle lever position for the aircraft control is calculated.

4.2.3 Vortex Controller

To cope with a vortex encounter a specific controller has been designed acting against the vortex induced moments before noticeable flight state deviations occur. In the following this controller is named "vortex controller" and it should be clear that the controller is controlling the encountering aircraft and not the vortex of the leading aircraft. The vortex controller consists of a feed-forward (FF) and a feedback (FB) part (Fig.11).

Considering the experience from the design of gust load alleviation systems and wind shear controllers [7, 8, 28] it is known that atmospheric disturbances can be treated best using FF control. This has the additional advantage of leaving the original aircraft behavior unchanged. Knowing the aerodynamics (including the control surface efficiency) of the respective aircraft to be controlled the necessary commands for compensation of the induced moments can be calculated. In the ideal case the FF

controller will fully compensate for the flow disturbances. But in a real system an additional FB controller is needed to cover real world effects and uncertainties.

4.4 Vortex Flow Measurement

For the presented investigation the measurement of the wake vortex flow was not addressed to be an issue. Nevertheless two different principles should be mentioned.

1. By means of LIDAR or LASER measurement systems placed in the nose of the aircraft the area on both sides in front of the wings can be scanned. The velocity field of the flow disturbances around the aircraft can be calculated by

$$\vec{V}_W = \vec{V}_K - \vec{V} . \qquad (9)$$

   The measurement ahead of the wing offers the advantage to compensate for system delays [7], e.g. computation delays.
2. Another kind of measurement can be performed by using an array of pressure ports along the wing span (minimum 4 per wing). The pressure variations induced by the vortex flow can be interpreted in terms of changed local lift coefficients from which the required control commands can be computed.

Whatever the principle of flow disturbance measurements is, it is important to know that the effects of interest show higher dynamics compared to the low dynamics of the normal aircraft motion. This offers the opportunity to filter out the relevant signal spectrum [7].

5 Aircraft Control in a Wake Vortex

There are different standards for separation distances established. In this paper the US IMC Separation Standards given in Tab.2 will be used. For the proposal of reduced but safe aircraft separations the underlaying physics have to be understood.

5.1 Steady Flight in a Wake Vortex

It is obvious that for parallel-like encounters the aircraft's roll response is the dominating motion. The worst case occurs when the wake vortex runs exactly parallel to the approach path and the following aircraft is permanent exposed to the vortex flow field in a quasi stationary flight. The areas to be avoided within a wake vortex flow field then can be calculated using the required control power normalized by the maximum available control power of the encountering aircraft expressed in terms of aileron deflection. The wake vortex induced roll moment can be compensated if

$$\left|\xi^*\right| = \left|\xi_{req}/\xi_{max}\right| < 1 \qquad (10)$$

applies. Depending on the combination of wake vortex generating and encountering aircraft areas of various threats can be defined by the normalized aileron deflection ξ^*.

The encountering aircraft is the Do128 (MTOW = 4.35t). As vortex generator two aircraft have been considered:

1) VFW614/ATTAS: MTOW = 20t
   initial circulation: $\Gamma_{L0} = 158 m^2/s$

2) generic aircraft: MTOW = 79t
   initial circulation: $\Gamma_{L0} = 342 m^2/s$.

Both pairings present a SMALL aircraft behind a LARGE one (see Tab.1). Aircraft 1) is at the lower and aircraft 2) is at the upper bound of the classification of "LARGE" aircraft. In principle both pairings show the same results concerning the encounter behavior except the fact that due to the lower initial circulation of combination 1) the threat vanishes earlier in this case. Therefore, this paper will focus on the latter combination since it is the more demanding case and covers the combination 2). Fig.12 illustrates the flow field behind the generic aircraft in terms of the amount of normalized aileron deflection $|\xi^*|$ at different separation distances. Assuming an approach speed of V_F = 60m/s for the follower aircraft the corresponding ages of the wake vortex are also listed in the table below:

SD [nm]	1.62	2.5	4.0	5.0	6.0
SD [km]	3.0	4.6	7.4	9.3	11.1
vortex age [s]	50	76.7	123.3	155.0	185.0
SD/ b_L [-]	88	135	217	273	326

In addition to the standard SDs the distance equivalent to the minimum runway occupation

time ROT = 50s is given which represents the absolute limit for aircraft separation.

In Fig.12 the red areas indicate that the required control power exceeds the available performance. In such a situation the aircraft cannot perform a steady flight. The displayed situations are true for neutral atmosphere and considering only aircraft self-induced turbulence (no atmospheric turbulence is present). These conditions can be regarded to be the worst case considering the vortex decay. In Figs. a) to c) it can be seen that the conditions do not change very much since only the diffusion phase has taken place and the rapid decay has not yet really developed. The required SD for the relevant aircraft combination is 4nm/7.4km. Even in this nominal situation red areas are still existent. The reasons why normally no wake vortex encounters are reported are: First, after the vortices came into existence they will start to sink down (initial sink rate for the vortices of the generic aircraft is $w_{sink} \approx 2$ m/s) and thus they will clear the approach path for the follower aircraft. Secondly, cross winds will shift the vortices away into lateral direction. Both effects normally prevent a full hit of the vortex core of a following aircraft. A pilot may interpret the penetration of the outer regions of the wake vortex as normal atmospheric turbulence.

Dependent on the accepted aileron deflection for vortex compensation it will take only some seconds until the situation becomes non-hazardous due to the wake vortex movement. Assuming that a control demand of $\xi^* < 0.3$ is tolerable this will happen in less than 30s.

The hazardous area of $\xi^* > 0.3$ can be roughly approximated by an ellipse or a rectangle as illustrated in Fig.12. The representative parameters versus SD of the approximated boundaries are given in Fig.13. For a SD of 6nm or more no hazardous areas of $\xi^* > 0.3$ do exist anymore. Together with the prediction of the wake vortex movement these simplified boundaries can be used to generate SDs as a function of tolerable normalized aileron deflections ξ^*.

For specific meteorological conditions the vortices will not move away fast enough or even can stay in the approach area. The shorter the SD the higher the risk of penetrating a hazardous area due to uncertainties in wake vortex behavior. For the acceptance of reduced SD it must be guaranteed that even unforeseen situations can be passed safely. This will only be possible by the support of automatic control.

5.2 Passing Through a Wake Vortex

In the real world a wake vortex encounter will be only a temporary but very dynamically event. A typical example for an unintended wake vortex encounter is represented by the following situation. The encountering SMALL aircraft is approaching the runway on a 3° glide slope and will penetrate the left vortex of a LARGE aircraft. The vortex line has a horizontal orientation and crosses exactly the glide slope. The SD is chosen to be 2.5 nm which is about 63% of the current standard.

Fig.14 shows the encounter with only the autopilot (designed for strong turbulence) active. When the vortex is penetrated the autopilot tries to keep the nominal flight path. Although the aileron deflection acts against the induced rolling momentum the aircraft experiences bank angles of about $+7° > \Phi > -13°$. In the beginning the aircraft banks to the right. Together with the lateral vortex velocity coming from the left it moves more than $y_g > 10$m to the right. There it is exposed to the strong downdraft between the two vortices and dives below the glide slope. After passing the vortex core (about 10s) the aircraft is recovered close to its nominal flight path.

In Fig.14 also the performance of the vortex controller is illustrated. It can be seen that the aircraft bank reaction $0° > \Phi > -2°$ can be neglected although stronger vortex velocities are encountered. But significant flight path deviations occur since the vortex controller is a state controller and not designed for flight path tracking. To overcome this deficiency it has to be combined with the autiopilot.

Fig.15 displays the results of the encounter using the combined autopilot and vortex controller. The results show little bank angle variations and satisfactory flight path deviations. But

to fulfill the task of flight path tracking and state control the required control power exceeds the available aileron capacity. If the applicable aileron deflection is limited to its realistic maximum ($|\xi^*| \leq 1$) the resulting aircraft behavior is deteriorated but still acceptable (Fig.15). Even the situation corresponding to the ROT (SD = 1.62nm) which leads to a SD of about 40% of the current nominal SD can be passed by automatic control (Fig.16)

It is clear that flying through the core of a vortex is the worst case that can happen and has to be avoided. As a result of the motion of the vortices such an extreme vortex encounter will be a very rare situation. But if this case occurs it can be coped by automatic control especially designed for this event. The exhibited aircraft behavior in terms of load factor might be uncomfortable but not hazardous. Much more dangerous are the high sink rates which occur when the down-wash between the vortex pair is penetrated. Especially close to ground such rates cannot be accepted. To make sure that no vortex encounter will happen in the vicinity of the ground an observation system is needed for sensing the space around the glide slope. From this information a prediction of the vortex motion in front of the runway can be derived.

More likely than hitting a vortex core will be penetrations of the outer vortex region. Fig.17 illustrates a flight a few meters left from the vortex line of the left vortex. The passed area (see Fig.12: yellow area) requires a normalized aileron deflection of $0.5 < |\xi^*| < 1$. The combined autopilot/vortex controller has no problem to keep the flight path and the aircraft states with only small variations although the maximum required normalized aileron deflection is about $\xi^* \approx -0.8$. Even close to the ground this aircraft behavior is acceptable.

6 Summary and Conclusions

The hazard of the velocity field of a wake vortex can be expressed by areas of normalized aileron deflections ξ^* required for permanent roll-momentum compensation in a quasi stationary flow field. According to the aircraft pairing, the actual weather dependent decay and the accepted deflection for vortex compensation, these areas can be approximated by the simple geometry of a rectangle or an ellipse. With regard to the vortex motion these simple bounds can be used to calculate SDs which provide non-hazardous conditions within the relevant space around the nominal approach path.

Vortices can be passed through even if the required control power temporarily exceeds the available capacity. This is possible since the extension of the cells of very high rotational velocities are limited to small areas. Therefore, the corresponding time of exposure is normally short. The necessary aileron deflection rates are high. A human pilot surprised by an unintended penetration will have problems to apply the correct control input amplitudes without phase delays [29]. This situation can be improved by an automatic controller especially designed to counteract the effects of vortices. The “vortex controller” introduced in this paper is well suited to cope with wake vortices in combination with an autopilot. It is mainly based on a disturbance feed-forward concept. This has got the advantage of leaving the aircraft control dynamics unchanged. Using forward looking information would allow to take control actions before the vortex penetration. This provides the potential for further controller improvements.

It is important to understand that the vortex controller is not designed to substitute a human pilot. The intention is to support the pilot and to relieve him from a high dynamic task. The vortex controller will compensate for the vortex induced disturbances and the pilot still has to control the aircraft. The situation can be compared with an active gust load alleviation system smoothing the aircraft’s gust response without interfering the pilot’s task.

The vortex controller is not thought to allow the disregard of the wake vortex hazard but it could be an element in the puzzle of reducing the SDs. An aircraft equipped with such a device should be able to follow another aircraft in a shorter SD since it is able to cope with unintended encounters which of course have to be an exception. It is proposed to reduce the currently applicable SDs in small steps to gather operational experience. In any case the resulting sepa-

ration distances have to be safe in terms of acceptable flight path excursions and flight state deviations.

7 References

[1] König R. Aircraft Response and Pilot Behaviour During a Wake Vortex Encounter Perpendicular to the Vortex Axis. *Flight in Adverse Environmental Conditions*, Gol, Norway, paper 17, pp 17/1-17/18, 1989.

[2] Hinton D A. Description of Selected Algorithms and Implementation Details of a Cocept-Demonstration Aircraft VOrtex Spacing System (AVOSS). NASA/TM-2001-211027, Hampton, Virginia, 2001.

[3] Gerz T. Wirbelschleppe – Minimierung, Vorhersage, Beobachtung und Erkennung von Wirbelschleppen ziviler Verkehrsflugzeuge. Projektplan, German Aerospace Center, 2001.

[4] de Bruin A et al. Assessment of Wake Vortex Safety –S-WAKE, ANNEX 1 "Description of Work", European Commission, Proj.No: G4RD-1999-0099, 1999.

[5] Ruitshauser D K and Cornelius J O'C. Aircraft Wake Vortex Spacing System (AVOSS) Performance Update and Validation Stud. NASA/TM-2001-211240, Hampton, Virginia, 2001.

[6] Frauenkron H et al. FLIP – Flight Performance Using Frankfurt ILS. DFS, German Air Navigation Services, Air Traffic Management Devision, 2001.

[7] König R and Hahn K U. Load Alleviation and Ride Smoothing Investigations Using ATTAS. *17th Congress of the International Council of the Aeronautical Sciences*, Stockholm, Sweden, pp 1379-1393, 1990.

[8] Hahn K U and König R. ATTAS Flight Test and Simulation Results of the Advanced Gust Management System LARS. *Atmospheric Flight Mechanics Conference*, Hilton Head Island, SC, pp 58-70, 1992.

[9] Krag B. S-WAKE Flight Test Report. Technical Note SWAKE-D-221_2_1, IB 111-2001/40, German Aerospace Center, Institute of Flight Research, Braunschweig, 2001.

[10] Sucipto T. Erweiterung eines Flugsimulationsprogramms auf einer UNIX-Workstation. *Konstruktiver Entwurf, TU Braunschweig, Institut für Flugführung*, Braunschweig, 1993.

[11] Dunkel W. An improved Model of a Propeller-Driven Type Aircraft. *1. Mathmod Vienna*, Wien, pp 918-921, 1993.

[12] Escande B and Aureche Y. Trailing Vortices and Safety. *CEAS/AAAF Forum "Research for Safety in Civil Aviation"*, Paris, 1999.

[13] Fischenberg D. Bestimmung der Wirbelschleppen-Charakteristik aus Flugmessdaten. *Deutscher Luft- und Raumfahrtkongress,* Stuttgart, Germany, 2002.

[14] Greene GC. An Approximate Model of Vortex Decay in the Atmosphere. *Journal of Aircraft,* Vol. 23, No. 7, pp 566-573, 1986.

[15] Han et al. Large Eddy Simulation of Aircraft Wake Vortices in a Homogeneous Atmospheric Turbulence: Vortex Decay and Decent. *AIAA 99-0756, 37th AIAA Aerospace Sciences Meeting and Exhibit„* Reno, 1999.

[16] Sarpkaya T. A New Model for Vortex Decay in the Atmosphere. *AIAA 99-0761, 37th AIAA Aerospace Sciences Meeting and Exhibit*, Reno, 1999.

[17] Donladson C snd Bilanin AJ. Vortex Wakes of Conventional Aircraft. *AGARDograph* No. 204, AGARD-AG-204, Princeton, 1975.

[18] Holzäpfel F. A Probabilistic Two-Phase Wake Vortex Decay and Transport Model. *Report No. 163,* German Aerospace Center, Institut für Physik der Atmosphäre, Oberpfaffenhofen, 2001.

[19] Campbell S D, Dasey T J, Freehart R E, Heinrichs R M, Matthews M P, Perras G H and Rowe G S. Wake Vortex Field Measurement Program at Memphis, TN, Data Guide. *Project Report NASA/L-2,* Lincoln Lab., MIT, Cambridge, MA, 1997.

[20] Oseen C W. *Arkiv för Mat., Astron. och Fys.,* Nr. 14, 1911.

[21] Lamb H. Hydrodynamics. Cambridge University Press, pp 590-592, Cambridge, 1932.

[22] Burnham D C and Hallock J N. Chicago Monostatic Acoustic Vortex Sensing System. Vol. 4, *Wake Vortex Decay*, Springfield, VA, National Information Service, 1982.

[23] Proctor F H. The NASA-Langley Wake Vortex Modelling Effort in Support of an Operational Aircraft Spacing System. *36th AIAA Aerospace Sciences Meeting and Exhibit*, AIAA 98-0589, Reno, 1998.

[24] Winckelmans G. Effect of non-uniform windshear onto vortex wakes: parametric models for operational systems and comparison with CFD studies. *4th WakeNet Workshop "Wake Vortex Encounter"*, Amsterdam, 2000.

[25] Holzäpfel F. Authors personnel correspondence on realistic wake vortex modeling, 2001.

[26] Gockel W. Design of an Autoland System for UAV Application Using ATTAS as Demonstrator. Institute of Flight Research, Report IB 111-2000/13, 2000.

[27] Lambregts A A. Integrated System Design for Flight and Propulsion Control Using Total Energy Principles. AIAA Paper 86-2143CP, 1986.

[28] Hahn K-U. Effect of Wind Shear on Flight Safety. *Progress in Aerospace Sciences*, Vol. 26, pp 225-259, 1989.

[29] Höhne G. A Model for the Pilot Behavior During Wake Vortex Encounters. *Report No. IB 111-2001/41,* German Aerospace Center, Institute of Flight Research, Braunschweig, 2001.

8 Figures and Tables

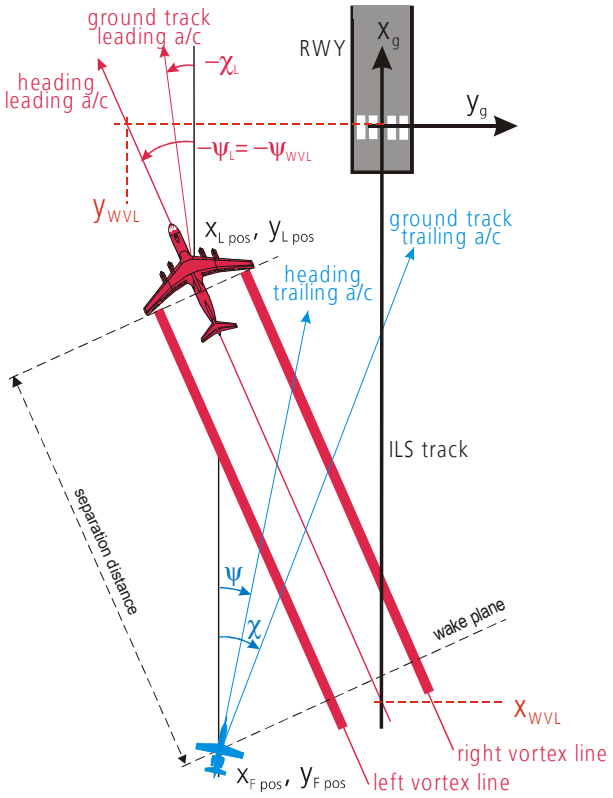

Fig.1: Encounter Scenario

CLASS	MASS
HEAVY	> 116 000 kg
B757	-
LARGE	> 18 600 kg
SMALL	≤ 18 600 kg

Tab.1: Aircraft Classification after FAA

Generator A/C	Follower A/C	Separation Minima
HEAVY	HEAVY	4 NM / 7.4 km
	LARGE	5 NM / 9.3 km
	SMALL	6 NM / 11.1 km
B757	HEAVY	4 NM / 7.4 km
	LARGE	4 NM / 7.4 km
	SMALL	5 NM / 9.3 km
LARGE	HEAVY	2.5 NM / 4.6 km
	LARGE	2.5 NM / 4.6 km
	SMALL	4 NM / / 7.4 km
SMALL	HEAVY	2.5 NM / 4.6 km
	LARGE	2.5 NM / 4.6 km
	SMALL	2.5 NM / 4.6 km

Tab.2: US Wake Vortex Separation for IMC

Fig.2: DLR's Advanced Technologies Testing Aircraft System VFW614 ATTAS

Fig.3: Smoke Generator Mounted on the Left Wing of ATTAS

Fig.4: Do128 Test Aircraft of the University of Braunschweig
(with courtesy of Institute of Flight Guidance of TU Braunschweig)

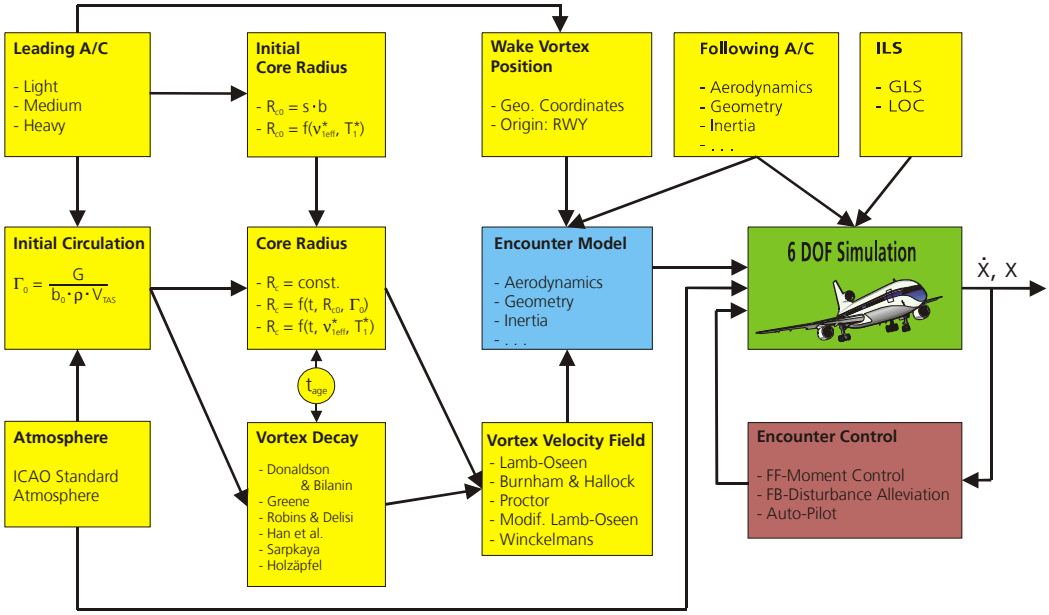

Fig.5: Block Diagram of nonlinear 6 DoF Encounter Simulation

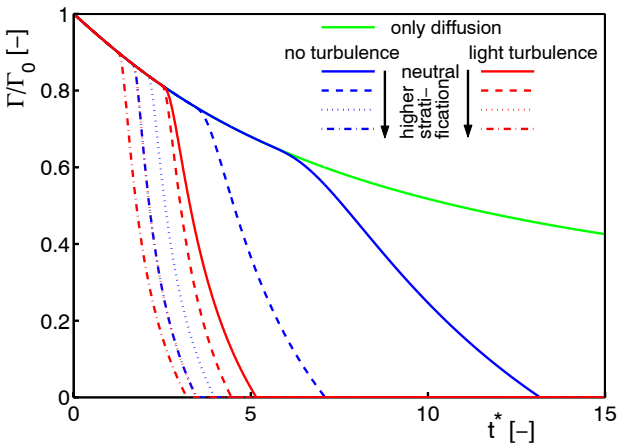

Fig.6: Circulation Strength Calculated by the P2P Model after HOLZÄPFEL [18]

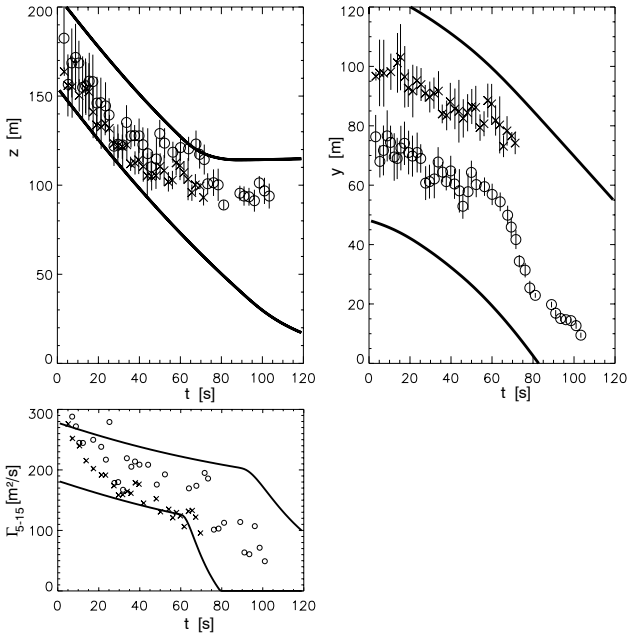

Fig.7: Uncertainty Bounds of the P2P Model Compared with Memphis Data (from [18])

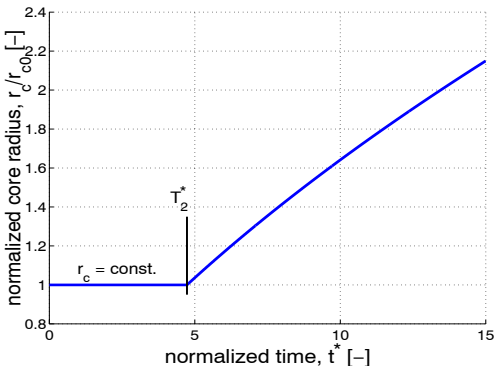

Fig.8: Development of Vortex Core Radius

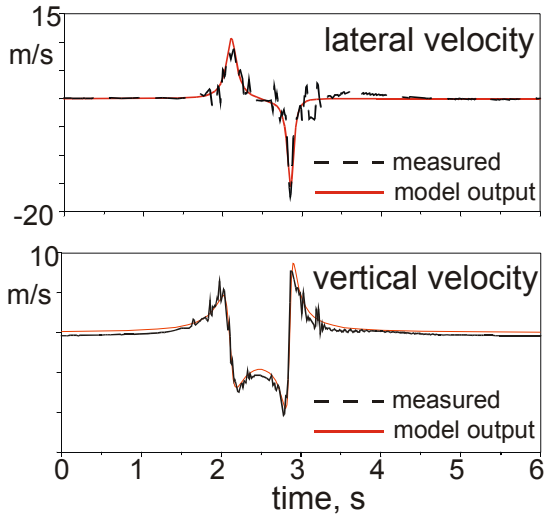

Fig.9: Comparison of Measured Velocity Field and Model Output (from [13])

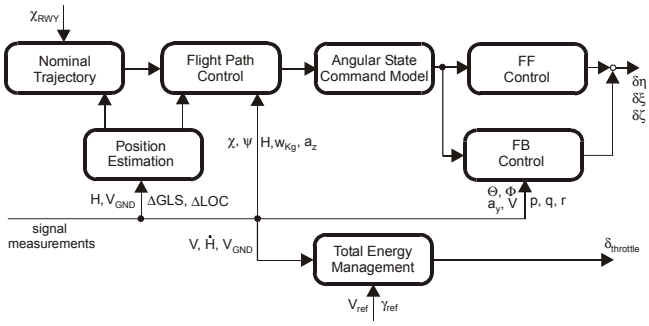

Fig.10: Block Diagram of Autopilot and Autothrottle

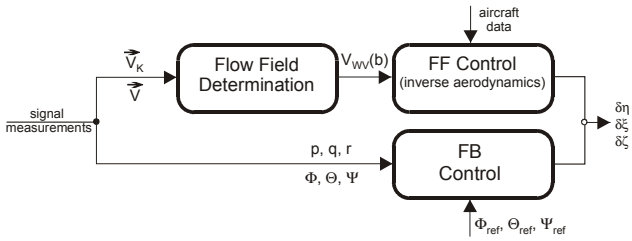

Fig.11: Block Diagram of Vortex Controller

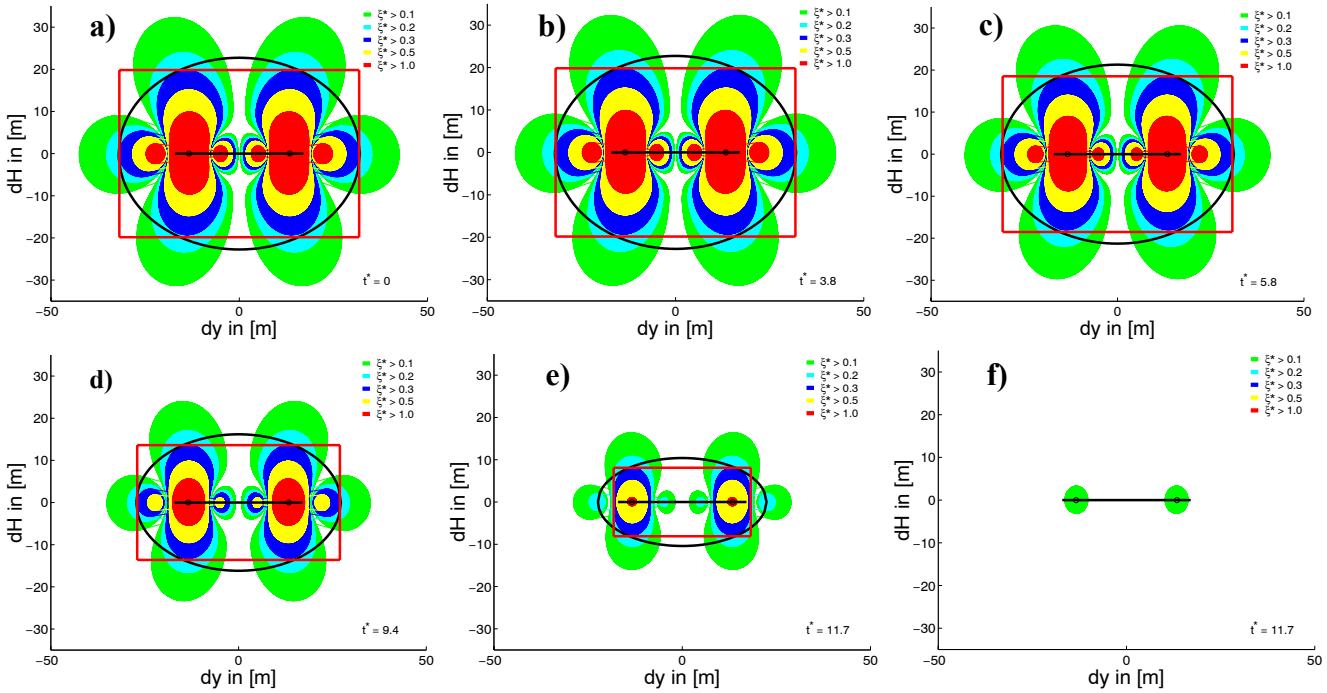

Fig.12: Required Aileron Deflection Behind a Vortex Generation Aircraft
(SMALL {4.35t} behind LARGE {79t})

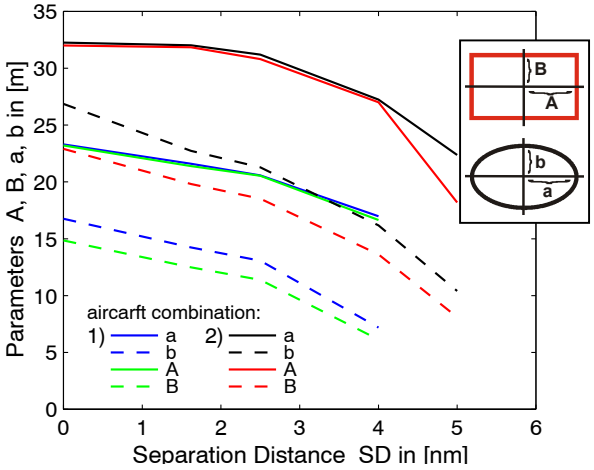

Fig.13: Parameters of the Hazard Boundary Approximations for $|\xi^*| \leq 0.3$
(SMALL {4.35t} behind LARGE {79t})

dimensions of the rectangle: A, B
semi-axes of the ellipse: a, b

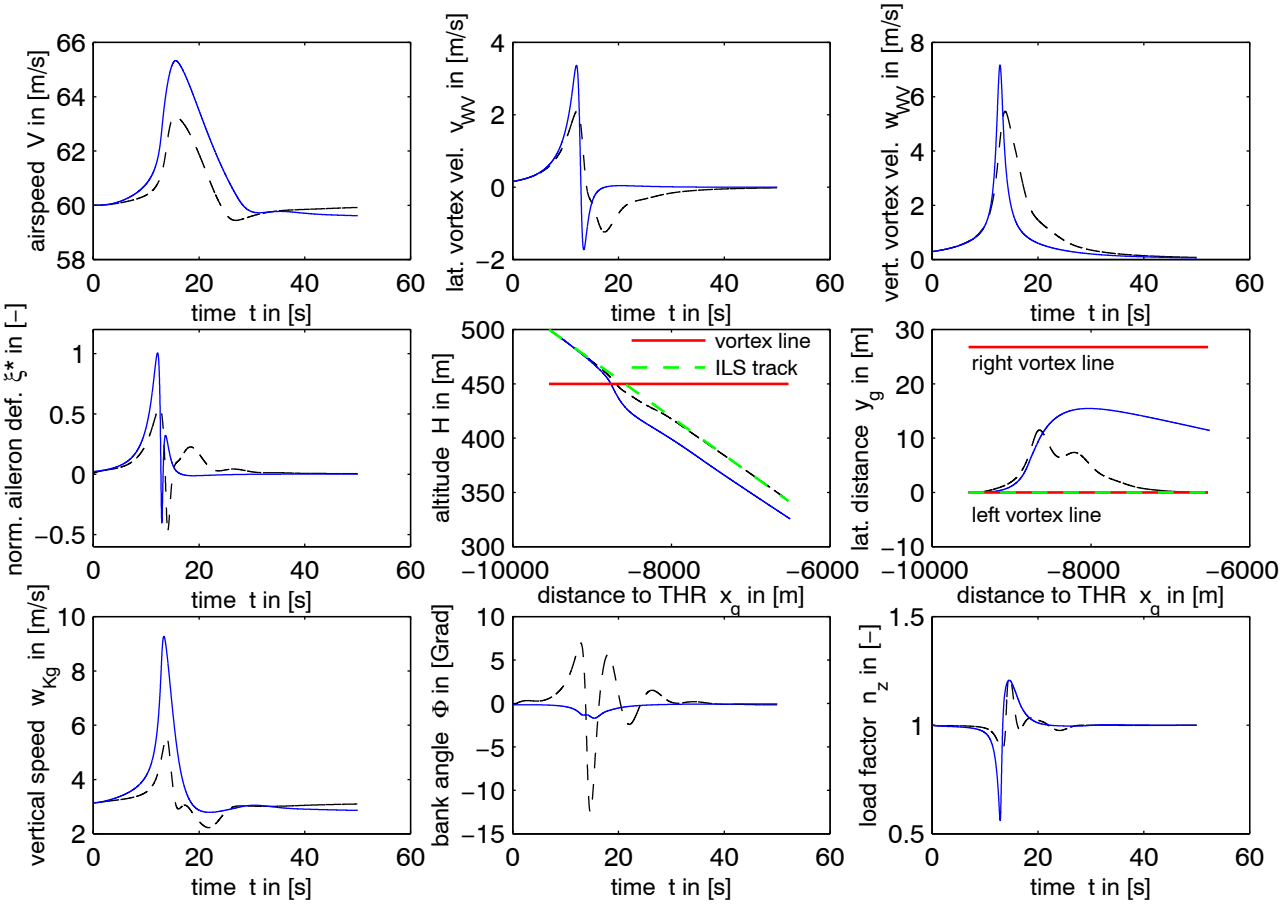

Fig.14: Wake Vortex Encounter Using Different Controllers (SMALL {4.35t} behind LARGE {79t})
- - - - autopilot —— vortex controller —— vortex lines - - - - ILS

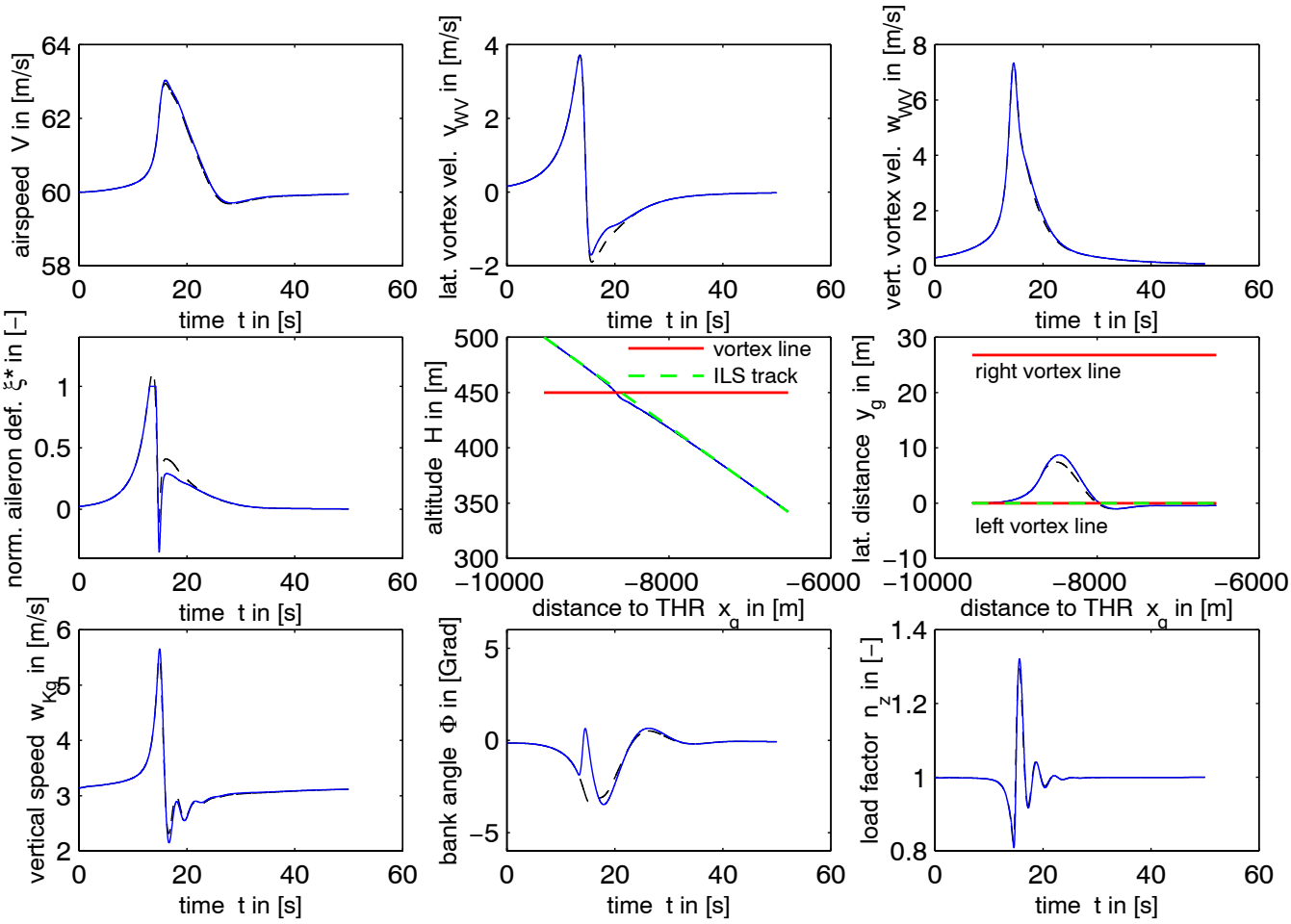

Fig.15: Wake Vortex Encounter Using Combined Autopilot and Vortex Controller
(SMALL {4.35t} behind LARGE {79t})

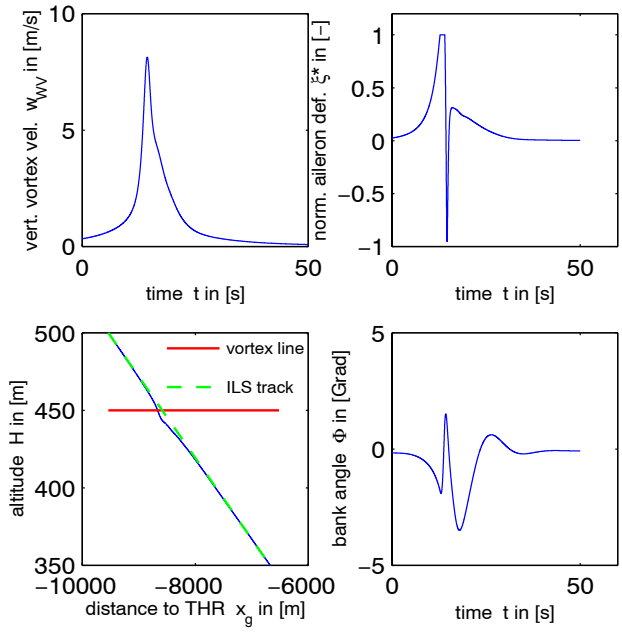

Fig.16: Encounter of a Wake Vortex with an Age of 50 Seconds (ROT)

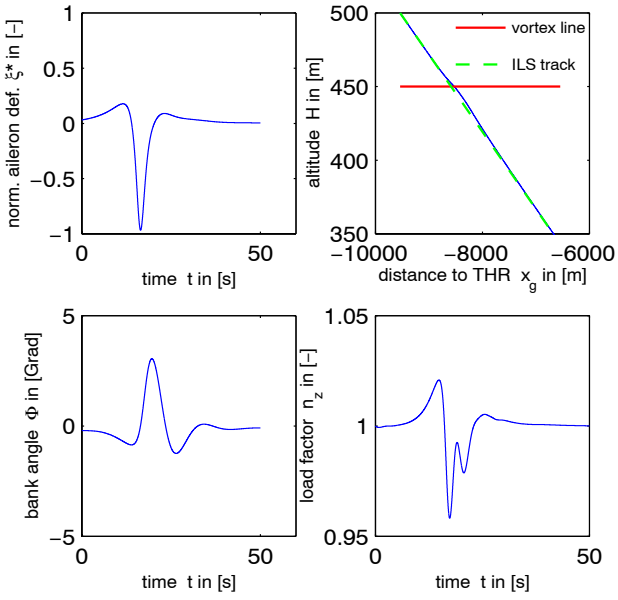

Fig.17: Wake Vortex Encounter Left of the Left Vortex Line
(Wake Vortex Age: 50s)